ISSN 1674-1056
http://cpb.iphy.ac.cn
http://iopscience.iop.org/cpb
中国物理 B
Chinese Physics
中国物理
Chinese Physics B

Terahertz coherent detection via two-color laser pulses of various frequency ratios

Xin-Yang Gu(顾新杨), Ke-Jia Wang(王可嘉), Zhen-Gang Yang(杨振刚), Jin-Song Liu(刘劲松)
Citation: Chin. Phys. B . 2019, 28(9): 098701 . **doi:** 10.1088/1674-1056/28/9/098701
Journal homepage: http://cpb.iphy.ac.cn; http://iopscience.iop.org/cpb

What follows is a list of articles you may be interested in

Effect of terahertz pulse on gene expression in human eye cells

Jin-Wu Zhao(赵晋武), Ming-Xia He(何明霞), Li-Jie Dong(东莉洁), Shao-Xian Li(李绍限), Li-Yuan Liu(刘立媛), Shao-Chong Bu(步绍翀), Chun-Mei Ouyang(欧阳春梅), Peng-Fei Wang(王鹏驰), Long-Ling Sun(孙珑玲)
Chin. Phys. B . 2019, 28(4): 048703 . **doi:** 10.1088/1674-1056/28/4/048703

Theoretical investigation of tunable polarized broadband terahertz radiation from magnetized gas plasma

Xin-Yang Gu(顾新杨), Jin-Song Liu(刘劲松), Zhen-Gang Yang(杨振刚), Sheng-Lie Wang(汪盛烈), Ke-Jia Wang(王可嘉)
Chin. Phys. B . 2018, 27(5): 058701 . **doi:** 10.1088/1674-1056/27/5/058701

Ultra-compact terahertz switch with graphene ring resonators

Jian-Zhong Sun(孙建忠), Le Zhang(章乐), Fei Gao(高飞)
Chin. Phys. B . 2016, 25(10): 108701 . **doi:** 10.1088/1674-1056/25/10/108701

Terahertz multi-metal-wire hybrid-cladding hollow waveguide for refractive index sensing

Ying-Ying Yu(于莹莹), Xu-You Li(李绪友), Kun-Peng He(何昆鹏), Bo Sun(孙波)
Chin. Phys. B . 2016, 25(2): 028703 . **doi:** 10.1088/1674-1056/25/2/028703

Performance analysis of LDPC codes on OOK terahertz wireless channels

Chun Liu(刘纯), Chang Wang(王长), Jun-Cheng Cao(曹俊诚)
Chin. Phys. B . 2016, 25(2): 028702 . **doi:** 10.1088/1674-1056/25/2/028702

Terahertz coherent detection via two-color laser pulses of various frequency ratios*

Xin-Yang Gu(顾新杨)[1], Ke-Jia Wang(王可嘉)[1], Zhen-Gang Yang(杨振刚)[2], and Jin-Song Liu(刘劲松)[1,†]

[1] *Wuhan National Laboratory for Optoelectronics, Huazhong University of Science and Technology, Wuhan* 430074, *China*
[2] *School of Optical and Electronic Information, Huazhong University of Science and Technology, Wuhan* 430074, *China*

(Received 18 June 2019; revised manuscript received 11 July 2019; published online 23 August 2019)

The mechanism of terahertz (THz) pulse coherent detection via two-color laser pulses of various frequency ratios in gas plasma is theoretically investigated. Our investigations demonstrate that except for the commonly used frequency ratio of 2, other uncommon frequency ratios can also be utilized to detect THz pulse, such as $2n$, $n+1/2$ ($n \leq 3$, n is a positive integer). The well-developed transient photocurrent model is extended to our terahertz detection process. Based on this model, our simulation results can be explained by analyzing the process of asymmetric electron ionization and electron acceleration.

Keywords: terahertz, gas plasma, coherent detection, photoionization

PACS: 87.50.U–, 52.25.Jm, 78.47.jh, 87.15.mn **DOI:** 10.1088/1674-1056/ab37fc

1. Introduction

Common THz detectors such as photoconductive antennas and electro–optic crystals cannot cover the entire THz range (0.1 THz–10 THz),[1–4] which are restricted by the carrier lifetime of photoconductors and the transverse-optic lattice oscillation in electro–optic crystals.[5] Fortunately, the broadband THz detection method with laser-induced gas plasma provides an approach to detect the entire THz range.[6–9] Except for broader detection bandwidth, the gas plasma has no phonon resonances or abrupt interfaces, and gas mediums do not have damage thresholds, making it a better choice for THz detection.

In 2006, Dai *et al.* firstly reported a broadband detection method of THz waves via terahertz-induced second harmonic (TISH) generation in a laser-induced gas plasma,[6] known as Air Breakdown Coherent Detection (ABCD) method. A phenomenological four-wave-mixing (FWM) model was used to explain their experimental phenomena that the probe laser intensity profoundly influenced the detection process.[10,11] The coherent detection requires high probe energies to obtain strong enough local oscillator second harmonic (SH) signal in their investigation, which can indirectly get the phase information of THz waves. Later, Karpowicz *et al.* utilized the ABCD method to detect THz radiation with the spectrum of approximately 20 THz.[7] In this method, a pair of electrodes was placed across the plasma to generate an external DC high voltage bias, which broke the symmetry of plasma and improved the dynamic detection range.

Recently, THz generation with two-color laser of various frequency ratios was reported by Wang *et al.*[12] Their particle-in-cell (PIC) simulation results indicate that two-color laser pulses with frequency ratios of $2n$, $n+1/2$, $n\pm1/3$ can radiate high-efficiency and stable THz waves. Furthermore, they successfully observed THz generation with two-color laser pulses of 400 nm+1600 nm and 800 nm+1200 nm,[13,14] experimentally demonstrating the THz generation with frequency ratios of 4:1 and 3:2. The FWM model could not explain their experimental phenomena with these frequency ratios. Instead, the transient photocurrent (PC) model first proposed by Kim *et al.* could well interpret the observed results and could also be utilized in the THz detection process.[15–17] The ionization-induced multiwave mixing model was proposed by Vvedenskii's group to explain the THz generation with uncommon laser frequency ratios.[18] Moreover, they experimentally generated the THz emission with two-color laser pulses of 800 nm+1600 nm for the first time.[19] Considering that the THz detection via laser-induced gas–plasma can be regarded as an inverse process of gas–plasma THz generation, the frequency ratios of two-color probe lasers in THz detection may have some corresponding properties. In 2015, a two-color THz detection method called Optically Biased Coherent Detection (OBCD) method was proposed by Li *et al.*,[20] requiring neither high energy nor DC high voltage bias. However, the frequency ratio of two-color probe laser was confined to 2 in their approach. Thus, the two-color THz detection with other uncommon frequency ratios should be systematically researched.

In this paper, the transient PC model is utilized to well explain the physical mechanism of ABCD and OBCD methods and our calculations are corresponding to the experimental results of Refs. [6] and [20]. Further, we extend the OBCD scheme to other frequency ratios of two-color probe lasers.

*Project supported by the National Natural Science Foundation of China (Grant Nos. 11574105, 61475054, and 61405063).
†Corresponding author. E-mail: jsliu4508@vip.sina.com
© 2019 Chinese Physical Society and IOP Publishing Ltd

Our study demonstrates that when frequency ratios of two-color probe laser are $2n$ and $n+1/2$ ($n \leq 3$, n is a positive integer), the THz coherent detection is high-efficiency, which is in concert with the conclusion in Ref. [13]. Besides, the simulation results are analyzed from the point of view of electron ionization and electron acceleration in detail. We find that the frequency ratios of $2n$ and $n+1/2$ significantly intensify the asymmetries of both electron ionization and electron acceleration, making the modulating effects of THz wave more evident than that with other frequency ratios. Further study reveals that the two series of efficient frequency ratios are applicable to different relative-phases. The frequency ratios $2n$ are efficient for THz detection with relative-phase $\Delta\varphi = m\pi$ (m is an integer), while the frequency ratios $n+1/2$ are efficient with relative-phase around $\Delta\varphi = m\pi/2$.

2. Theoretical model

The well-developed transient PC model can interpret the experiment results of the ABCD and OBCD schemes. The PC model includes two processes: electron ionization and electron acceleration in gas plasma, forming an oscillating current J. This oscillating current leads to the radiation of electromagnetic waves with various frequencies, written as[15–17]

$$E_{\text{out}}(t,\Delta t) \propto \frac{\mathrm{d}J(t,\Delta t)}{\mathrm{d}t} \propto \left(E_{\text{pro}}(t)+E_{\text{THz}}(t+\Delta t)\right)N_{\text{e}}(t,\Delta t), \quad (1)$$

where $E_{\text{pro}}(t)$ and $E_{\text{THz}}(t+\Delta t)$ are the probe field and incident THz field, respectively. Δt is the time interval between probe laser pulse and THz pulse and $N_{\text{e}}(t,\Delta t)$ is the plasma density, which is calculated via the static tunneling (ST) model in this paper.[21] We use a filtering and inverse Fourier transform to obtain the narrow-band signal at a specific frequency, *i.e.*, SH ($2\omega_0$) signal in the ABCD and OBCD schemes:

$$E_{2\omega_0}(t,\Delta t) \propto \int_{-\infty}^{+\infty} f_{2\omega_0}(\omega)\,\mathrm{e}^{\mathrm{i}\omega t}\mathrm{d}\omega \times \int_{-\infty}^{+\infty} E_{\text{out}}(t',\Delta t)\,\mathrm{e}^{-\mathrm{i}\omega t'}\mathrm{d}t', \quad (2)$$

where $f_{2\omega_0}(\omega)$ is an SH narrow-band pass filter function. Then the SH intensity $I_{2\omega_0}$ can be easily calculated, which is proportional to the THz electric field E_{THz}. It should be noted that the calculated SH intensity $I_{2\omega_0}$ in PC model is always greater than zero because it contains an SH background radiation $I^{\text{LO}}_{2\omega_0}$, which can be experimentally filtered out by using a lock-in amplifier.[6] Thus, a DC SH intensity should be subtracted from $I_{2\omega_0}$ to obtain the detected intensity $I^{\text{T}}_{2\omega_0}$, $I^{\text{T}}_{2\omega_0}$=$I_{2\omega_0} - I^{\text{LO}}_{2\omega_0}$.

In our simulation, the probe lasers have a Gaussian formation with center wavelength $\lambda = 800$ nm, full width at half maximum (FWHM) $T_{\text{FWHM}} = 30$ fs and focal beam radius $w_0 = 10$ μm. Note that FWHM represents the temporal width of laser pulses. The gas medium is nitrogen and its density is assumed to be 2.4×10^{19} cm^{-3}. Figure 1(a) depicts the incident THz field with a 9.4×10^6-V/m peak field. In the ABCD scheme, the detected SH intensity is unipolar and the detection is incoherent when single probe pulse energy is 60 μJ, as shown in Fig. 1(b), corresponding to the experimental results with low probe energy in Ref. [6]. In order to coherently detect THz field and obtain its phase information, one should enhance the probe pulse energy in ABCD scheme or employ the two-color method (called OBCD scheme) with low probe energy. The relative phase difference between two lasers $\Delta\varphi$ is zero. Figure 1(c) depicts the detected SH intensity in OBCD scheme, in which both fundamental (800 nm) and SH (400 nm) probe pulse energy are 60 μJ with the same FWHM and focal beam radius in our simulation. Compared with ABCD scheme, one can see that the two-color method can explore higher SH intensity with lower probe energy, which is also corresponding to the experimental results in Ref. [20].

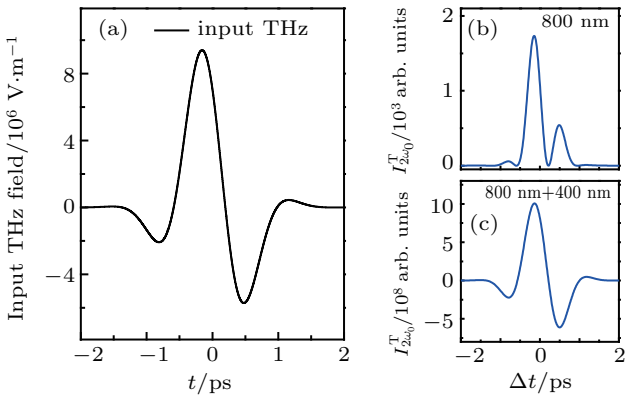


Fig. 1. (a) Input THz wave. (b) Detected SH intensity in ABCD scheme. (c) Detected SH intensity in OBCD scheme.

When we change the frequency ratios of two-color probe lasers in OBCD scheme, total electric field at the plasma center can be written as $E_{\text{pro}}(t) = E_{\omega_1}(t) + E_{\omega_2}(t)$, where $E_{\omega_1}(t)$ is the fundamental probe field but $E_{\omega_2}(t)$ is no longer the SH probe field. We assume $\omega_1 < \omega_2$ and thereby ω_2/ω_1 is always larger than one in our following calculations. In order to confirm the detection frequency with other uncommon frequency ratios, we utilize the transient PC model to calculate several cases with two special frequency ratios ($\omega_2/\omega_1 = 3/2$, 4), which have been experimentally demonstrated the THz generation in Ref. [13]. Figure 2(a) plots the calculated signal intensities *versus* different detection frequencies with two-color probe lasers of 1200 nm+800 nm and 800 nm+533.3 nm ($\omega_2/\omega_1 = 3/2$). We find that the maximums of detected intensities are at the frequency of ω_2, corresponding to 800 nm and 533.3 nm, respectively. Furthermore, the cases of two-color probe lasers of 1600 nm+400 nm and 800 nm+200 nm ($\omega_2/\omega_1 = 4$) are depicted in Fig. 2(b). Similarly, the maximums of detected intensities are also at the frequency of

ω_2 (corresponding to 400 nm and 200 nm) with $\omega_2/\omega_1 = 4$. Hence, the frequency at ω_2 is the most sensitive detected frequency. The multi-wave mixing model can also support these results.[6,10] With $\omega_2/\omega_1 = 3/2$ and 4 in THz generation, THz energy scales with $(I_{\omega_1})^3 (I_{\omega_2})^2$ and $(I_{\omega_1})^4 (I_{\omega_2})$, where I_{ω_1} and I_{ω_2} are energies of the two-color lasers. As the inverse process of gas–plasma THz generation, THz detection must have the corresponding property that the detected intensity at the frequency of ω_2 should be more sensitive to THz wave than that at ω_1. Therefore, we explore the incident THz field by measuring the radiation intensity at frequency of ω_2 in OBCD scheme with different frequency ratios. The narrow-band signal at a frequency of ω_2 can be expected to vary as

$$E_{\omega_2}(t,\Delta t) \propto \int_{-\infty}^{+\infty} f_{\omega_2}(\omega)\, \mathrm{e}^{\mathrm{i}\omega t}\mathrm{d}\omega \times \int_{-\infty}^{+\infty} E_{\mathrm{out}}(t',\Delta t)\, \mathrm{e}^{-\mathrm{i}\omega t'}\mathrm{d}t'. \quad (3)$$

The intensity of detected frequency can be calculated as $I_{\omega_2}(\Delta t) \propto \int_{-\tau/2}^{\tau/2} [E_{\omega_2}(t,\Delta t)]^2 \mathrm{d}t$, where τ is the probe pulse duration. Note that a DC signal $I_{\omega_2}^{\mathrm{LO}}$ should also be subtracted from I_{ω_2} to obtain the detected intensity $I_{\omega_2}^{\mathrm{T}}$, $I_{\omega_2}^{\mathrm{T}} = I_{\omega_2} - I_{\omega_2}^{\mathrm{LO}}$.

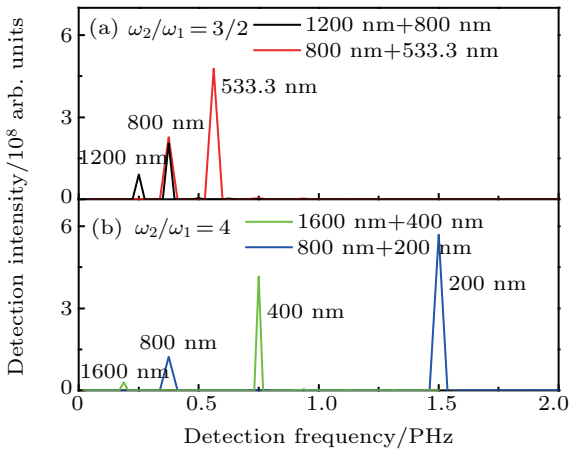


Fig. 2. Calculated signal intensities *versus* different detection frequencies with (a) two-color probe lasers of 1200 nm+800 nm and 800 nm+533.3 nm (frequency ratio $\omega_2/\omega_1 = 3/2$); (b) two-color probe lasers of 1600 nm+400 nm and 800 nm+200 nm (frequency ratio $\omega_2/\omega_1 = 4$).

3. Two-color detection with different frequency ratios

To investigate the frequency ratios of two-color probe lasers in OBCD scheme, we fix the fundamental probe laser at frequency $\omega_1 = 375$ THz (corresponding to wavelength $\lambda_1 = 800$ nm) and explore the incident THz field by measuring the radiation at frequency of ω_2. The two laser pulses have the same duration $T_{\mathrm{FWHM}} = 30$ fs and energy $W = 60$ μJ. Figure 3(a) plots the calculated signal intensities $I_{\omega_2}^{\mathrm{T}}$ with four different frequency ratios ($\omega_2/\omega_1 = 2$, 4, 3/2, 5/2). We can find that except the commonly used frequency ratio of 2, other uncommon frequency ratios can also be utilized to retrieve THz pulses, such as $\omega_2/\omega_1 = 4, 3/2, 5/2$. Although detected signal intensities with $\omega_2/\omega_1 = 4$, 3/2, 5/2 are less than that with $\omega_2/\omega_1 = 2$, the intensities are still considerable. Moreover, there are no distortions of detected waves and the detected waves are well coincident with input THz wave (green dot lines) with these frequency ratios. However, when $\omega_2/\omega_1 = 3$ and 5, the signal intensities $I_{\omega_2}^{\mathrm{T}}$ decrease approximately 4000 times compared with $\omega_2/\omega_1 = 2$, making detection inefficient. More than that, the waveforms of $I_{\omega_2}^{\mathrm{T}}$ become unipolar and cannot retrieve the input THz electric-field, as shown in Fig. 3(b).

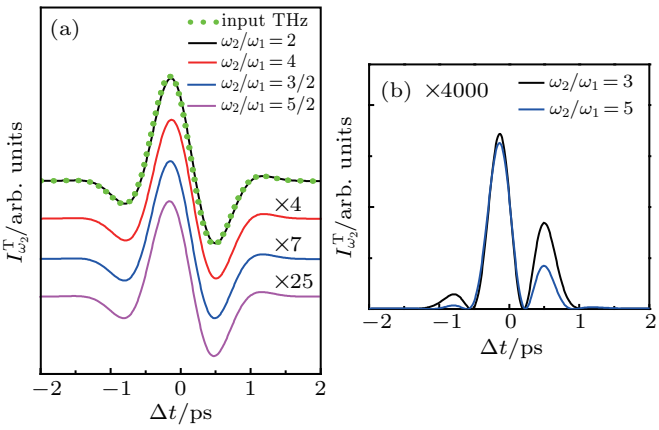


Fig. 3. Calculated temporal waveforms of signal intensities at frequency of ω_2 with different frequency ratios (a) $\omega_2/\omega_1 = 2$, 4, 3/2, and 5/2; (b) $\omega_2/\omega_1 = 3$ and 5.

To further investigate the frequency ratios of two-color probe lasers in OBCD scheme, we change the second probe laser frequency ω_2 in the range from ω_1 to $6.5\omega_1$. The two laser pulses have the same durations $T_{\mathrm{FWHM}} = 30$ fs, 40 fs, 50 fs and energy $W = 60$ μJ. The relative phase difference $\Delta\varphi$ is zero. Figure 4(a) displays the peaks of signal intensities $I_{\omega_2}^{\mathrm{T}}$ *versus* the frequency ratios of two-color probe lasers, which are proportional to the peak values of detected THz field strengths. It is clearly seen that peak values of curves in Fig. 4(a) appear at $\omega_2/\omega_1 = 3/2$, 2, 5/2, 7/2, 4, 6 with three different durations of the laser pulses. Compared with these specific frequency ratios, the detected signal intensities of other frequency ratios are slight and negligible. In addition, one can find in Fig. 4(a) that the detected intensity is significantly affected by FWHM. The wider FWHM is, the stronger detected signal is. Moreover, to further evidence these frequency ratios, we also fix the fundamental probe laser with wavelength $\lambda_1 = 1200$ nm and 1600 nm and change frequency ratios ω_2/ω_1 from 1 to 6.5. It can still be observed that the peaks of detected signal intensities appear at these frequency ratios, as shown in Fig. 4(b). Without a doubt, these specific frequency ratios must be regular that $\omega_2/\omega_1 = 2n$, $n + 1/2$ (n is a positive integer).

Next we study three series of frequency ratios $\omega_2/\omega_1 = 2n$, $n + 1/2$, and $n \pm 1/3$. It can be observed that the peaks

of $I^{\mathrm{T}}_{\omega_2}$ are detected efficiently in series of $\omega_2/\omega_1 = 2n$ and $n+1/2$ with three different wavelengths λ_1 of first probe laser ($\lambda_1 = 800$ nm, 1200 nm, and 1600 nm), as illustrated in Figs. 4(c) and 4(d). Note that the curves with three different λ_1 show the similar tendencies, but the peaks of $I^{\mathrm{T}}_{\omega_2}$ become very weak when n is greater than 3. However, unlike the previous reports in Ref. [12], the peaks of $I^{\mathrm{T}}_{\omega_2}$ are relatively weak in series of $\omega_2/\omega_1 = n \pm 1/3$ and there are no obvious rules, as shown in Fig. 4(e). This is because in the THz generation model in Ref. [12], the authors directly calculated the generated THz waves, but we measure THz waves indirectly by detecting the signal intensity at frequency of ω_2 in the THz detection process. As a consequence, our calculations reveal that the signal intensities $I^{\mathrm{T}}_{\omega_2}$ can be detected efficiently in two series of frequency ratios $\omega_2/\omega_1 = 2n$ and $n+1/2$ ($n \leq 3$, n is a positive integer).

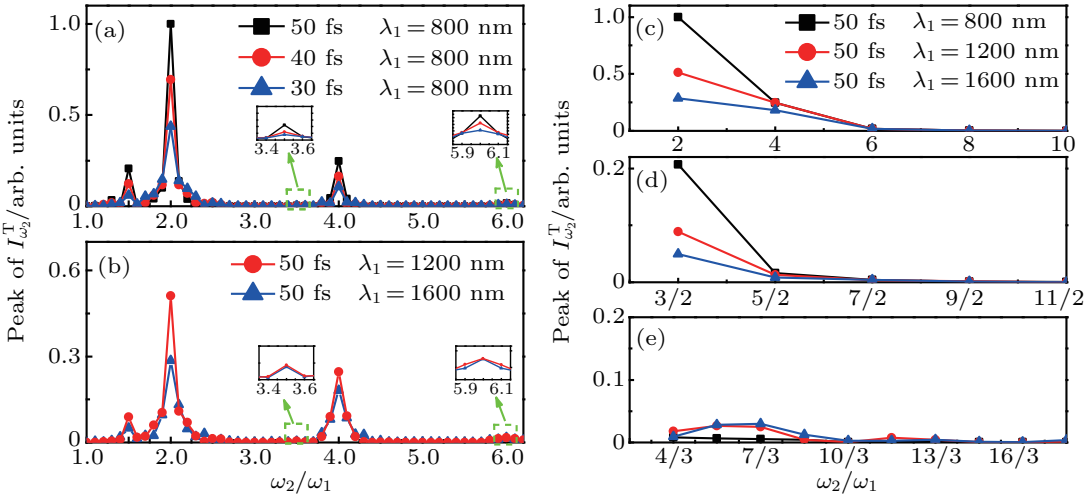


Fig. 4. Calculated signal peak intensities at frequency of ω_2 as a function of the frequency ratios of two-color probe lasers with (a) different FWHMs (30 fs, 40 fs, and 50 fs) and same fundamental probe lasers (800 nm). (b) Same FWHM (50 fs) and different fundamental probe lasers (1200 nm and 1600 nm). Insets: amplified curves around the frequency rates $\omega_2/\omega_1 = 3.5$ and 6. (c)–(e) Calculated signal peak intensities at frequency of ω_2 *versus* three series of frequency ratios $\omega_2/\omega_1 = 2n$, $n+1/2$, and $n \pm 1/3$ with the same FWHM (50 fs) and different fundamental probe lasers (800 nm, 1200 nm, and 1600 nm).

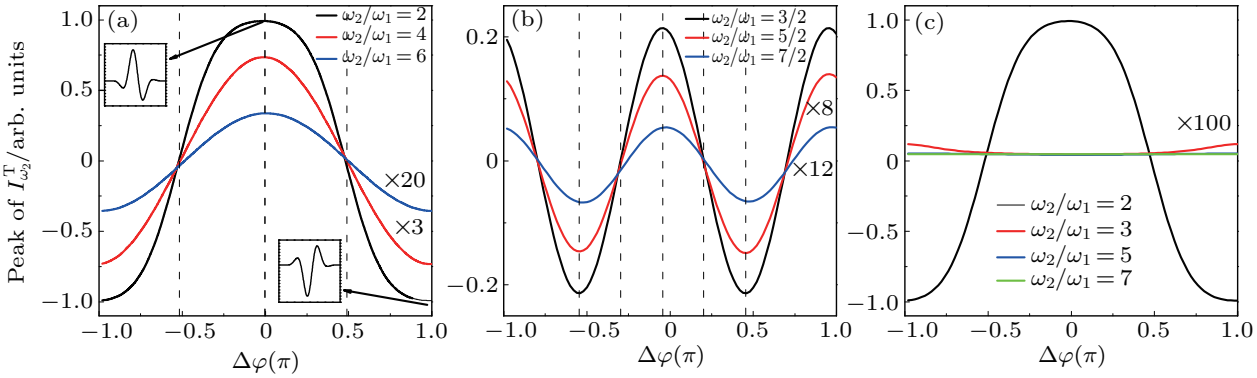


Fig. 5. Peak of signal intensities $I^{\mathrm{T}}_{\omega_2}$ *versus* the relative-phase $\Delta\varphi$ of two lasers with frequency rates (a) $\omega_2/\omega_1 = 2n$. (b) $\omega_2/\omega_1 = n+1/2$ ($n \leq 3$). (c) $\omega_2/\omega_1 = 2, 3, 5, 7$. The insets in panel (a) are the temporal waveforms of $I^{\mathrm{T}}_{\omega_2}$ with $\omega_2/\omega_1 = 2$ when $\Delta\varphi = 0$ and π.

The relative phase difference between two laser pulses $\Delta\varphi$ plays a crucial role in the process of THz generation and detection. Next we study influence of relative-phase $\Delta\varphi$ of two laser pulses in OBCD scheme. In this calculation, we fix the fundamental probe laser at frequency $\omega_1 = 375$ THz (corresponding to $\lambda_1 = 800$ nm), and study two series of frequency rates $\omega_2/\omega_1 = 2n$, $n+1/2$ ($n \leq 3$), and inefficient frequency ratios ($\omega_2/\omega_1 = 3, 5, 7$). The two laser pulses have the same duration $T_{\mathrm{FWHM}} = 50$ fs and energy $W = 60$ μJ. Figures 5(a) and 5(b) plot peaks of signal intensities $I^{\mathrm{T}}_{\omega_2}$ *versus* the relative-phase $\Delta\varphi$ of two lasers in the case of $\omega_2/\omega_1 = 2n$ and $n+1/2$, respectively. One can find that both peaks of $I^{\mathrm{T}}_{\omega_2}$ with two series of frequency rates have cosinoidal dependences on the $\Delta\varphi$. However, their variation periods are different. When $\omega_2/\omega_1 = 2n$, variation periods of the peaks of $I^{\mathrm{T}}_{\omega_2}$ are 2π. The extreme points of curves in Fig. 5(a) are $\Delta\varphi = 0$ and $\pm\pi$, and the polarities of corresponding detected THz waves are inversed (see insets in Fig. 5(a)). When $\omega_2/\omega_1 = n+1/2$, variation periods of the peaks of $I^{\mathrm{T}}_{\omega_2}$ became π. The extreme points of curves in Fig. 5(b) are $\Delta\varphi = -0.04\pi$, $\pm\pi - 0.04\pi$, and $\pm 0.5\pi - 0.04\pi$. Figure 5(c) plots peaks of signal intensities $I^{\mathrm{T}}_{\omega_2}$ *versus* the relative-phase with inefficient frequency ratios. We can find that regardless of the relative-phase $\Delta\varphi$, the peaks of $I^{\mathrm{T}}_{\omega_2}$ with inefficient frequency ratios (the curves

have been amplified 100 times) are always much less than the maximum of peak of $I^{\mathrm{T}}_{\omega_2}$ with $\omega_2/\omega_1 = 2$. Namely, the influence of relative-phase to the detection efficiency of inefficient frequency ratios is much weaker than the case of $\omega_2/\omega_1 = 2n$, $n+1/2$.

Note that the efficient frequency ratios $\omega_2/\omega_1 = 2n$, $n+1/2$ are not always applicable to all relative-phases. For instance, when $\Delta\varphi = \pm 0.5\pi$, the frequency ratios $\omega_2/\omega_1 = 2n$ are inefficient for THz detection, which is corresponding to the results in Ref. [20]. But the frequency ratios $\omega_2/\omega_1 = n+1/2$ are still efficient for THz detection, as shown in Fig. 5(b). Therefore, the two series of efficient frequency ratios are applicable to different relative-phases. The frequency ratios $\omega_2/\omega_1 = 2n$ are efficient for THz detection with relative-phase $\Delta\varphi = m\pi$ (m is an integer), while the frequency ratios $\omega_2/\omega_1 = n+1/2$ are efficient with relative-phase around $\Delta\varphi = m\pi/2$. Hence, the relative-phase of two probe lasers should be controlled to be $m\pi$ or $m\pi/2$ when we apply these two series of efficient frequency ratios. A pair of fused silica wedges can be used to experimentally control the relative-phase by finely adjusting the mechanical step size of wedges.[20,22]

4. Explanations by electron ionization and acceleration

It is well known that the asymmetric electron ionization and electron acceleration play remarkable roles in the whole THz detection process. Thus, in the following, we explain our results of THz detection with different frequency ratios from these points. Since pulse width of femtosecond probe lasers is much shorter than that of ps-THz pulse, the incident THz pulse can be regarded as a constant field during the duration time of one laser pulse, modulating the electron ionization and acceleration.

We use the static tunneling model to analyze ionization processes with frequency ratios of 2, 4, 3/2, 5/2, and 3, which represent the efficient frequency ratios of $2n$, $n+1/2$ and inefficient frequency ratios for THz detection, respectively. We let the relative-phase of two-color lasers $\Delta\varphi = 0$. Figures 6(a)–6(e) illustrate the time derivative of plasma density $\mathrm{d}N_\mathrm{e}/\mathrm{d}t$ (black line) and plasma density N_e (blue line) during the time of one fs-laser pulse with peak THz electric field modulating gas plasma. In Figs. 6(a)–6(e) we fix the probe lasers with the same energy $W_1 = W_2 = 60$ μJ and FWHM $T_{\mathrm{FWHM}} = 50$ fs at various frequency ratios, which causes the identical saturated numbers of electrons N_e via gas ionization (see blue lines). Nevertheless, the distributions of their ionization points are different. And it is clear that the greater value of ω_2/ω_1 is, the larger number of ionization points is in one cycle of probe laser pulse.

To further investigate the modulating properties of THz pulse, we plot $\Delta\mathrm{d}N_\mathrm{e}/\mathrm{d}t$ after subtracting the time derivative of plasma density without a modulation of THz wave in Fig. 6(f)–6(j), denoted as $\Delta\mathrm{d}N_\mathrm{e}/\mathrm{d}t = \mathrm{d}N_\mathrm{e}^{\omega_{1,2}+T}/\mathrm{d}t - \mathrm{d}N_\mathrm{e}^{\omega_{1,2}}/\mathrm{d}t$. In Fig. 6(f) with $\omega_2/\omega_1 = 2$, we can observe that the THz wave promotes electron ionization at the first five ionization points and then suppresses ionization at the following ionization points. Here we assume the symmetry of $\Delta\mathrm{d}N_\mathrm{e}/\mathrm{d}t$ with respect to the center of two adjacent ionization points, so the curve at two adjacent ionization points is asymmetric in Fig. 6(f). Likewise, the modulation effects of THz wave are asymmetric when $\omega_2/\omega_1 = 3/2$, 5/2, and 4, as illustrated in Figs. 6(g)–6(i). In contrast, the polarities of curves at two adjacent ionization points are always opposite as shown in Fig. 6(j). It means that the modulation effects of THz wave is approximately periodic symmetric with $\omega_2/\omega_1 = 3$. Summing up the above, when the frequency ratios of two-color probe lasers are $2n$, $n+1/2$, the incident THz wave can intensify the asymmetry in electron ionization process.

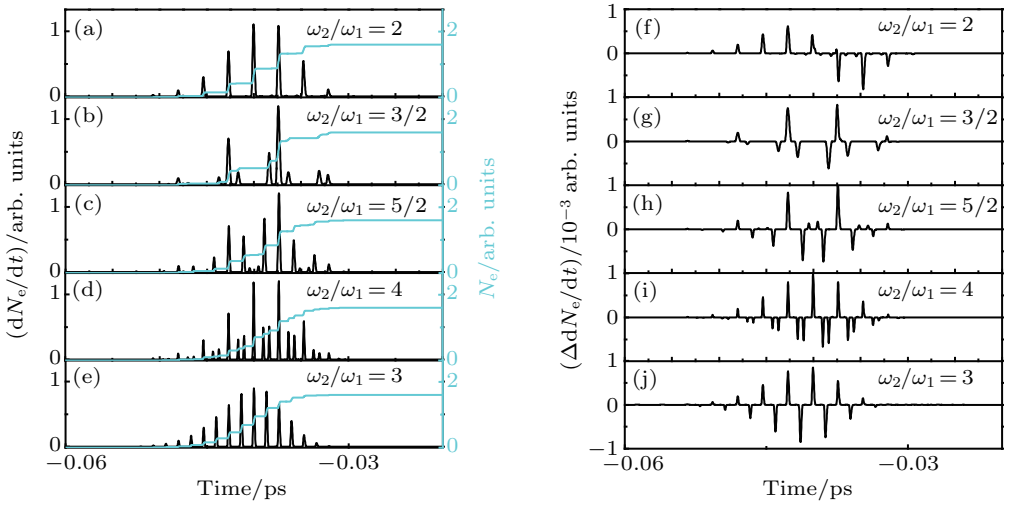


Fig. 6. In the case of peak THz electric field modulating plasma during the time of one fs-laser pulse, (a)–(e) time derivative of plasma density $\mathrm{d}N_\mathrm{e}/\mathrm{d}t$ (black line) and plasma density N_e (blue line) with various frequency ratios; (f)–(j) variation of time derivative of plasma density $\Delta\mathrm{d}N_\mathrm{e}/\mathrm{d}t$ after subtracting the case without a modulation of THz wave with various frequency ratios.

As mentioned above, the radiation field from gas plasma is proportional to the time derivative of oscillating current, written as $E_{\rm out}(t) \propto {\rm d}J(t)/{\rm d}t$. Thus we plot the time derivative of oscillating current with various frequency ratios, which are periodic as shown in Figs. 7(a)–7(e). In Fig. 7(a) with $\omega_2/\omega_1 = 2$, ${\rm d}J(t)/{\rm d}t$ formed within the first half cycle are greater than the ones within the followed half cycle. Here we assume the symmetry of ${\rm d}J(t)/{\rm d}t$ with respect to the center of one oscillation cycle, so the curve in Fig. 7(a) is asymmetric. Similarly, ${\rm d}J(t)/{\rm d}t$ with $\omega_2/\omega_1 = 3/2$, 5/2, and 4 all have varying degrees of asymmetry. However, ${\rm d}J(t)/{\rm d}t$ with $\omega_2/\omega_1 = 3$ is approximately periodic symmetric (see Fig. 7(e)), which causes the radiation fields at frequency ω_2 with $\omega_2/\omega_1 = 2n$, $n+1/2$ are greater than the ones with other frequency ratios.

To study the modulating effects of incident THz wave to oscillating currents, the detailed analyses are performed as follows. The $\Delta{\rm d}J(t)/{\rm d}t$ in the peak and valley positions of incident THz wave with $\omega_2/\omega_1 = 2$ and 3 are plotted in Figs. 7(f) and 7(g), respectively, where $\Delta{\rm d}J/{\rm d}t = {\rm d}J^{\omega_{1,2}+T}/{\rm d}t - {\rm d}J^{\omega_{1,2}}/{\rm d}t$. By analyzing these two figures, it can be observed that when the signs of the incident THz fields are opposite, their modulating effects to ${\rm d}J(t)/{\rm d}t$ are completely opposite, indicating that the intensities of emission from plasma center with different incident THz intensities at frequency of ω_2 are totally different and the information of THz wave can be effectively encoded into emission at frequency of ω_2. Therefore, the intensity of emission at frequency ω_2 can resolve both positive and negative fields in a real THz wave, coherent detecting the bipolar THz wave. Furthermore, the incident THz wave with $\omega_2/\omega_1 = 2$ has much huger influence over ${\rm d}J(t)/{\rm d}t$ than the case of $\omega_2/\omega_1 = 3$, indicating that the incident THz wave with $\omega_2/\omega_1 = 2$ significantly intensifies the asymmetry of electron acceleration, but its influences are slight when $\omega_2/\omega_1 = 3$. In other words, we can infer that the modulating effects of THz wave to oscillating currents with $\omega_2/\omega_1 = 2n$ and $n+1/2$ are much more significant than those with other frequency ratios.

Therefore, figures 6 and 7 reveal that the frequency ratios $\omega_2/\omega_1 = 2n$ and $n+1/2$ (with the same relative-phase $\Delta\varphi = 0$) significantly intensify the asymmetries of both electron ionization and electron acceleration, making the THz detection more efficient than that with other frequency ratios.

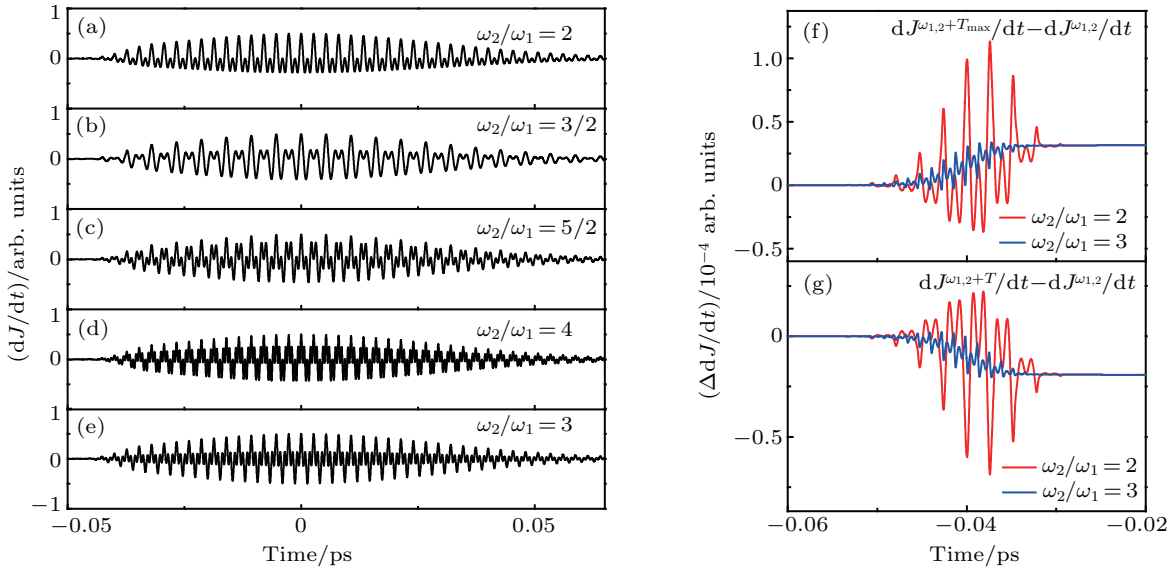


Fig. 7. (a)–(e) Time derivative of oscillating current ${\rm d}J/{\rm d}t$ with various frequency ratios in the case of peak THz electric field modulating plasma during the time of one fs-laser pulse. (f) and (g) Variation of time derivative of oscillating current $\Delta{\rm d}J/{\rm d}t$ in the peak and valley positions of incident THz wave with $\omega_2/\omega_1 = 2$ and 3, respectively.

Next, we study the electron ionization and electron acceleration with different relative-phases of two probe lasers. As example, figure 8 illustrates the time derivative of plasma density ${\rm d}N_{\rm e}/{\rm d}t$ and variation of time derivative of plasma density $\Delta{\rm d}N_{\rm e}/{\rm d}t$ with $\Delta\varphi = 0$ and π /2 when $\omega_2/\omega_1 = 2$. We can find from Fig. 8(a) that the amplitude of ${\rm d}N_{\rm e}/{\rm d}t$ with $\Delta\varphi = 0$ is bigger than that with $\Delta\varphi = \pi$ /2, but the number of ionization points with $\Delta\varphi = \pi$ /2 is larger than that with $\Delta\varphi = 0$. It makes the saturated numbers of ionized electrons identical. By analyzing Fig. 8(b), we can find that the curve of $\Delta{\rm d}N_{\rm e}/{\rm d}t$ is asymmetric with $\Delta\varphi = 0$. However, $\Delta{\rm d}N_{\rm e}/{\rm d}t$ becomes approximately periodic central symmetric when $\Delta\varphi = \pi/2$. It can prove that the symmetry of electron ionization significantly depends on the relative-phase of two probe lasers when the frequency ratio is same.

Figures 9(a) and 9(b) give the time derivative of oscillating current ${\rm d}J(t)/{\rm d}t$ with $\Delta\varphi = 0$ and π /2 when frequency ratio is fixed at 2. It is clear that ${\rm d}J(t)/{\rm d}t$ formed within the first half cycle are greater than the ones within the followed half cycle with $\Delta\varphi = 0$, so the curve in Fig. 9(a) is asymmet-

ric. However, $\mathrm{d}J(t)/\mathrm{d}t$ with $\Delta\varphi = \pi/2$ is approximately periodic central symmetric as shown in Fig. 9(b). Moreover, when $\omega_2/\omega_1 = 2$, the incident THz wave with $\Delta\varphi = 0$ has much huger influence over $\mathrm{d}J(t)/\mathrm{d}t$ than the case of $\Delta\varphi = \pi/2$, as shown in Fig. 9(c), which makes the THz detected intensity with $\Delta\varphi = 0$ greater than that with $\Delta\varphi = \pi$ /2.

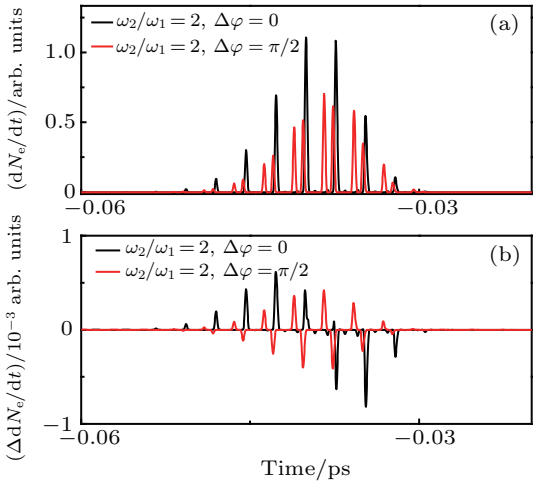


Fig. 8. In the case of peak THz electric field modulating plasma during the time of one fs-laser pulse, (a) time derivative of plasma density $\mathrm{d}N_e/\mathrm{d}t$ and (b) variation of time derivative of plasma density $\Delta\mathrm{d}N_e/\mathrm{d}t$ after subtracting the case without a modulation of THz wave with relative-phases $\Delta\varphi = 0$ and $\pi/2$ when $\omega_2/\omega_1 = 2$.

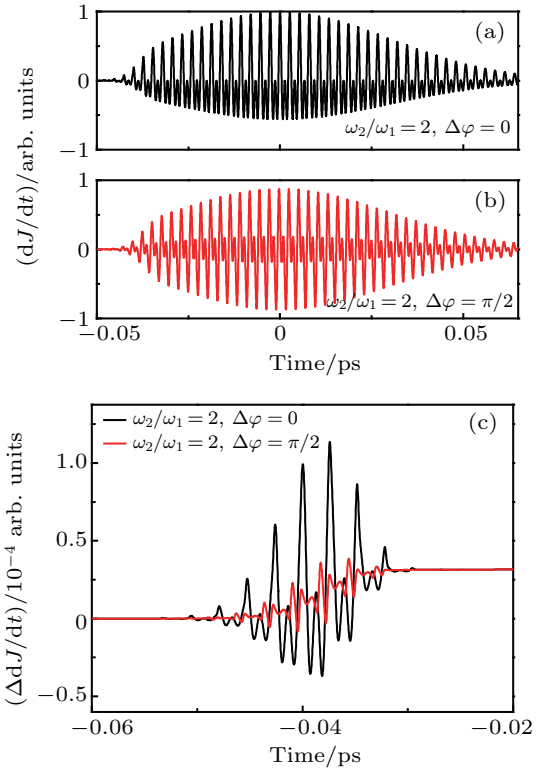


Fig. 9. In the case of peak THz electric field modulating plasma during the time of one fs-laser pulse: (a) and (b) time derivative of oscillating current $\mathrm{d}J/\mathrm{d}t$, (c) variation of time derivative of oscillating current $\Delta\mathrm{d}J/\mathrm{d}t$ with relative-phases $\Delta\varphi = 0$ and $\pi/2$ when frequency ratio is fixed at 2.

As a consequence, we can infer from Fig. 8 and Fig. 9 that the symmetries of electron ionization and electron acceleration both significantly depend on the relative-phase of two probe lasers when the frequency ratio is the same, which is also consistent with the result in Fig. 5. The frequency ratios $\omega_2/\omega_1 = 2n$ are efficient for THz detection with relative-phase $\Delta\varphi = m\pi$ (m is an integer), while the frequency ratios $\omega_2/\omega_1 = n + 1/2$ are efficient with relative-phase around $\Delta\varphi = m\pi/2$.

5. Conclusions

In summary, we systematically investigated the THz pulse coherent detection via two-color laser pulses of various frequency ratios in gas plasma. With two series of frequency ratios $\omega_2/\omega_1 = 2n$ and $n + 1/2$ ($n \leq 3$, n is a positive integer), the THz pulse can be coherent detected effectively, which are demonstrated in cases of different fundamental probe laser ($\lambda_1 = 800$ nm, 1200 nm, 1600 nm) and FWHM ($T_{\mathrm{FWHM}} =$ 30 fs, 40 fs, 50 fs). Furthermore, the well-developed transient PC model can support our simulation results. We extend this PC model to two-color THz detection process and provide an approach to explore two-color THz detection with specific frequency ratios. From the points of view of the electron ionization and acceleration, we find that the frequency ratios $\omega_2/\omega_1 = 2n$ and $n + 1/2$ significantly intensify the asymmetries of both electron ionization and electron acceleration, making the modulating effects of THz wave more evident than that with other frequency ratios. Hence, the THz detection is more efficient with $\omega_2/\omega_1 = 2n$ and $n + 1/2$. Our further study reveals that the relative-phase of two probe lasers also affects detection efficiency. The frequency ratios $\omega_2/\omega_1 = 2n$ are efficient for THz detection with relative-phase $\Delta\varphi = m\pi$ (m is an integer), while the frequency ratios $\omega_2/\omega_1 = n + 1/2$ are efficient with relative-phase around $\Delta\varphi = m\pi/2$.

Nowadays, various reported THz sources are excited by uncommon fundamental fs-lasers[23–25] or lasers with uncommon frequency ratios.[13,18,26] Compared with traditional electro–optic sampling or photoconductive antenna detection schemes, THz detection via laser-induced gas plasma has greater detected intensity and wider spectrum width (cover the entire THz band). Consequently, this two-color detection method with uncommon frequency ratios is an alternative detection method in theoretical and experimental researches.

References

[1] Schmuttenmaer C A 2004 *Chem. Rev.* **104** 1759
[2] Leitenstorfer A, Hunsche S, Shah J, Nuss M C and Knox W H 1999 *Appl. Phys. Lett.* **74** 1516
[3] Dietz R J B, Globisch B, Roehle H, Stanze D, Göbel T and Schell M 2014 *Opt. Lett.* **22** 19411
[4] Oguchi K, Iwasaki H, Okano M and Watanabe S 2016 *Appl. Phys. Lett.* **108** 011105
[5] Zhang X C and Xu J 2010 *Introduction To THz Wave Photonics* (New York: Springer-Verlag) pp. 27–48
[6] Dai J, Xie X and Zhang X C 2006 *Phys. Rev. Lett.* **97** 103903
[7] Karpowicz N, Dai J, Lu X, Chen Y, Yamaguchi M, Zhao H and Zhang X C 2008 *Appl. Phys. Lett.* **92** 011131

[8] Dai J, Clough B, Ho I C , Lu X, Liu J and Zhang X C 2011 *IEEE Trans. Terahertz Sci. Technol.* **1** 274
[9] Dai J, Liu J and Zhang X C 2011 *IEEE J. Sel. Top. Quantum Electron.* **17** 183
[10] Cook D J and Hochstrasser R M 2000 *Opt. Lett.* **25** 1210
[11] Bartel T, Gaal P, Reimann K, Woerner M and Elsaesser T 2005 *Opt. Lett.* **30** 2805
[12] Wang W M, Sheng Z M, Li Y T, Zhang Y and Zhang J 2017 *Phys. Rev. A* **96** 023844
[13] Zhang L L, Wang W M, Wu T, Zhang R, Zhang S J, Zhang C L, Zhang Y, Sheng Z M and Zhang X C 2017 *Phys. Rev. Lett.* **119** 235001
[14] Wang W M, Zhang L L, Li Y T, Sheng Z M and Zhang J 2018 *Acta Phys. Sin.* **67** 124202 (in Chinese)
[15] Kim K Y, Glownia J H, Taylor A J and Rodriguez G 2007 *Opt. Express* **15** 4577
[16] Kim K Y 2009 *Phys. Plasmas* **16** 056706
[17] Wang H, Wang K, Liu J, Dai H and Yang Z 2012 *Opt. Express* **20** 19264
[18] Kostin V A, Laryushin I D, Silaev A A and Vvedenskii N V 2016 *Phys. Rev. Lett.* **117** 035003
[19] Vvedenskii N V, Korytin A I, Kostin V A, Murzanev A A, Silaev A A and Stepanov A N 2014 *Phys. Rev. Lett.* **112** 055004
[20] Li C Y, Seletskiy D V, Yang Z and Sheik-Bahae M 2015 *Opt. Express* **23** 11436
[21] Corkum P B, Burnett N H and Brunel F 1989 *Phys. Rev. Lett.* **62** 1259
[22] Dai J, Karpowicz N and Zhang X C 2009 *Phys. Rev. Lett.* **103** 023001
[23] Lee S H, Lu J, Lee S J, Han J H, Jeong C U, Lee S C, Li X, Jazbinšek M, Yoon W, Yun H, Kang B J, Rotermund F, Nelson K A and Kwon O P 2017 *Adv. Mater.* **29** 1701748
[24] Kang B J, Baek I H, Lee S H, Kim W T, Lee S J, Jeong Y U, Kwon O P and Rotermund F 2016 *Opt. Express* **24** 11054
[25] Mingardi A, Zhang W D, Brown E R, Feldman A D, Harvey T E and Mirin R P 2018 *Opt. Express* **26** 14472
[26] Zhang S, Zhang L L, Wu T, Zhao H and Yu X M 2017 *Terahertz Emit. Receiv. Appl. VIII*, August 23, 2017, San Diego, California, USA, p. 103830E